Secondary structure of the 5′-region of *PGY1/MDR1* mRNA

Elena V. Kostenko[a], Robert Sh. Beabealashvilly[b], Valentin V. Vlassov[a], Marina A. Zenkova[a,*]

[a] *Novosibirsk Institute of Bioorganic Chemistry, Siberian Division of Russian Academy of Sciences, 8 Lavrentiev Ave., Novosibirsk 630090, Russia*
[b] *Institute of Experimental Cardiology, Cardiology Scientific Centre, Russian Academy of Medical Sciences, Moscow 121552, Russia*

Received 7 February 2000; received in revised form 11 May 2000

Edited by Masayuki Miyasaka

Abstract In order to identify the optimal target sites for antisense oligonucleotides in the human multiple drug resistance mRNA, the secondary structure of the 5′-terminal part of this mRNA (nucleotides 1–678) was investigated. By using results of probing with ribonucleases T1, ONE and V1 and results of computer simulations, a model of the 5′-region of the *PGY1/MDR1* mRNA was built. The molecule is formed by three major domains comprising several hairpins separated by single-stranded fragments. The predicted single-stranded regions of the *PGY1/MDR1* mRNA efficiently bind complementary oligonucleotides.

Key words: RNA structure; *PGY1/MDR1*; Antisense oligonucleotide

1. Introduction

Multidrug resistance (MDR) associated with simultaneous development of cellular cross-resistance to the structurally and functionally unrelated lipophilic drugs is the major obstacle for cancer chemotherapy [1]. This phenotype is characterized by overexpression of the *PGY1/MDR1* gene, which encodes a plasma membrane 170 kDa glycoprotein, called P-glycoprotein (P-gp) [2]. P-gp is assumed to act as an energy-dependent drug-efflux pump involved in the control of cellular drug accumulation. Attempts to circumvent MDR are often focused to inhibitors of a P-gp function. It is known that many agents including the calcium channel blocker verapamil [3], immunosuppressor cyclosporin A [4] and oestrogen antagonist tamoxifen can circumvent the MDR [5,6]. However, the clinical use of these compounds has its limitation as the toxicity and lack of specificity [7].

Antisense oligonucleotides are considered as promising therapeutics capable of down regulating specific gene expressions [8]. Attempts have been made to use the antisense approach to overcome the cellular MDR [9–11], however the tested oligonucleotides did not show sufficient inhibiting activity.

Selection of target sequences for antisense oligonucleotides in mRNA is the key step in the development of antisense constructs. Existing approaches to computing RNA structure do not provide unambiguous predictions of optimal targets in RNAs for antisense oligonucleotides. The currently used approaches are based on the empirical screening of a great number of oligonucleotides and on testing of oligonucleotides binding to RNA detected by various techniques: gel shift analysis [12] or binding to oligonucleotide arrays [13–15]. The oligonucleotides hybridization sites can be revealed by ribonuclease (RNase) H digestion [10,16–18]. In spite of the fact that combinatorial and semi-combinatorial approaches are potentially powerful and allow simultaneous assessment of a great number of oligonucleotides within the given RNA sequence [14], all these methods are limited by various factors as the hybridization conditions [13], the complexity of obtained oligonucleotide pools [17], and steric problems arising from the hybridization of structured RNAs with oligonucleotide arrays [19].

To develop antisense oligonucleotides to *PGY1/MDR1* mRNA, we investigated the structure of the 5′-proximal region of this mRNA by enzymatic probing and built a model of this RNA using the probing and computer simulations data. We have found that the single-stranded sequences predicted by our model are accessible for complementary oligonucleotides. The proposed mRNA structure explains the data of early studies on targeting *PGY1/MDR1* RNA with oligonucleotides.

2. Materials and methods

2.1. Oligonucleotides

Oligonucleotides 130-RT 5′-CCATCCCGACCTCG (complementary sequence 130–143), 240-RT 5′-GACTGACAGTTG (235–246), 340-RT 5′-CACCAGCATCATG (341–353), 450-RT 5′-CCTCCAGATTCATG (452–465), 560-RT 5′-GTCTTCCAGCTGCC (554–566), 660-RT 5′-AGACATCATCTGTAAG (659–678), AS-1 5′-GACCTCGCGCTCCTTG (122–137), AS-2 5′-CATTGCGGTCCCCTTC (150–165), AS-3 5′-GTCCAGCCCCATGGA (319–333) were synthesized by standard phosphoramidite chemistry and purified by ion-exchange and reverse-phase high performance liquid chromatography. The oligonucleotides were homogeneous as assayed by 15% polyacrylamide gel electrophoresis (PAGE) in denaturing conditions followed by staining with Stains-All [20].

2.2. Enzymatic probing of the in vitro transcript of the PGY1/MDR1 mRNA fragment

The 678 nucleotides *PGY1/MDR1* mRNA fragment (one *PGY1/MDR1* mRNA transcription initiation site), corresponding to nucleotides −140 to +538 (+1 is the A of the P-gp translation initiation codon), was obtained by in vitro transcription using T7 RNA polymerase and plasmid pMDR-670 [21], linearized with restriction enzyme *Sma*I, as a template, according to the protocol described in [22]. The transcript was purified by size-exclusion chromatography using 'Speen-column' (Sigma), ethanol-precipitated and dissolved in MilliQ water.

In vitro transcript of *PGY1/MDR1* mRNA was probed with RNase T1 [23], RNase ONE [24] and RNase V1 [25] (Promega). Reactions were carried out at 25°C in 20 μl 50 mM HEPES, pH 7.0, containing 200 mM KCl, 5 mM $MgCl_2$, 200 μg/ml in vitro transcript *PGY1/*

*Corresponding author. Fax: (7)-3832-333677.
E-mail: marzen@niboch.nsc.ru

PII: S0014-5793(00)01650-1

MDR1 mRNA and 1 mg/ml total yeast tRNA as carrier. Incubation time was 15 min for RNase ONE (0.03–0.5 U/ml) and T1 (0.05–1 U/ml), and 10 min for RNase V1 (0.01–0.5 U/ml).

Sites of enzymatic cleavages were determined by primer-directed reverse transcription as described in [26] using 5′-^{32}P-labeled oligonucleotides 130-RT, 240-RT, 340-RT, 450-RT, 560-RT and 660-RT, as primers. The products of primer extension were fractionated on 6% or 8% polyacrylamide gel containing 8 M urea.

2.3. Prediction of the PGY1/MDR1 mRNA secondary structure

RNA secondary structures were calculated using MFOLD subroutine of the GCG software package [27,28] based on free energy minimization algorithm. Calculations were performed at 37°C.

2.4. Hybridization of in vitro transcript of PGY1/MDR1 mRNA with antisense oligonucleotides

Binding of oligonucleotides AS-1, AS-2, AS-3 to the in vitro transcript of the *PGY1/MDR1* mRNA was investigated using a fluorometric titration assay at 37°C in 50 mM HEPES pH 7.5, containing 5 mM $MgCl_2$, 200 mM KCl, 0.5 mM EDTA. Oligonucleotides were 5′-end-labeled with pyrene according to described procedures [29]. Pyrene was excited at 343 nm and fluorescence emission was monitored at 382 nm using an MPF4 Hitachi spectrofluorimeter. Upon stoichiometric binding of pyrene-labeled oligonucleotide to RNA, pyrene fluorescence increases allowing to determine the equilibrium binding constant according to a modified Shtern–Folmer equation [30].

3. Results

The investigated 678 nucleotides in vitro transcript of the *PGY1/MDR1* mRNA includes the 5′-non-coding regulatory region (−140; −1), P-gp translation initiation codon and a fragment of the coding region (+1; +538). To identify single-stranded and double-stranded sequences in this RNA, we investigated cleavage of the RNA with RNases ONE and T1 and RNase V1. The cleavage patterns were visualized by primer-directed reverse transcription followed by electrophoresis of the cDNA products [26]. In order to detect positions on the template at which the reverse transcriptase pauses or stops artefactually incubation controls were processed in parallel with the samples treated with RNases. Some of these stops are thought to be the result from spontaneous RNA hydrolysis, which occurs most frequently at pyrimidine–adenine phosphodiester bonds and may show intrinsic fragility of RNA at these sites [31]. Others are probably due to pausing of the reverse transcriptase in highly structured regions of the RNA template [26]. Representative autoradiographs of the structure probing experiments are shown in Fig. 1.

Three alternative folds of the 5′-proximal 678 nucleotides of the *PGY1/MDR1* mRNA were obtained by computer simulation. The secondary structure model that maximally fits the experimental data is shown in Fig. 2. The RNA chain folds into a hairpin structure that forms three distinct domains: domain I comprises nucleotides 1–280, domain II is formed by nucleotides 281–569 and domain III by nucleotides 570–678 (Fig. 2).

Domain I includes three hairpins containing 8–20 nucleotides long terminal and internal loops. The stem-loop structure (nucleotides 1–53) consists of helix (8–19/53–42) closed by a large loop (20–41). Although positions 20–41 are sensitive to RNases T1 and ONE scissions, the possibility of base-pairing within this loop cannot be excluded. Nucleotides 54–228 form the long stem-loop structure containing double-stranded regions sensitive to RNase V1 (54–61/221–228, 65–74/208–218, 87–94/176–183) and several internal loops (75–86, 95–110) reactive to RNases ONE and T1 as shown in Fig. 1. The P-gp translation initiation site is located within the hexanucleotide terminal loop sensitive to RNases T1 and ONE (nucleotides 137–144). In addition, the mentioned positions, sequences 118–130, 151–154, 161–179, 229–237, 242–254, 261–269, display the sensitivity to RNases T1 and ONE and represent potential target sites for antisense oligonucleotides in this domain (Fig. 2).

Domain II is connected to domain I by a single-stranded sequence (281–292). Domain II seems to be highly structured which is indicated by a number of RNase V1 cuts found within this region. Nucleotides 293–300/310–317, 318–323/333–338, 416–419/353–359 (Fig. 1D) form helices cut by RNase V1. These structures contain sites sensitive to RNases ONE and T1 cleavage (positions 281–292, 301–310, 324–332, 360–366, 380–383, 387–396, 434–442, 454–471, 499–502).

A-U-rich domain III seems to have a very loose structure. In this domain, the probing experiments did not reveal any definite structure elements. All tested nucleases produced diffuse cleavage patterns and a number of artefactual reverse transcriptase stops. According to computer modeling, residues 570–634 may form a stem-loop structure containing bulged bases and internal loops. Only nucleotides 591–594 and 641–646 seem to form stable helices.

For targeting the *PGY1/MDR1* mRNA, we used the following antisense oligonucleotides: AS-1, complementary to residues 122–137 (corresponding to nucleotides −4 to +16, where +1 is A in AUG codon), AS-2, complementary to residues 150–165 (+10 to +25), and AS-3, complementary to nucleotides 319–334 (+178 – +194) (Fig. 2). We designed these antisense oligonucleotides taking into account our data [32,33] and data of other studies [34] evidencing that oligonucleotides bind to the structures where effective formation of nucleation complexes is possible. The nucleation complex can be formed with 4–6 nucleotides long single-stranded sequences [32] with further invasion of the oligonucleotide into RNA structure and formation of extended heteroduplex.

We investigated hybridization of the chosen oligonucleotides to *PGY1/MDR1* mRNA by fluorescence-monitored titration of the 5′-end pyrene-labeled antisense oligonucleotides with an increasing concentration of RNA. It is known that the fluorescence of pyrene-labeled oligonucleotides is strongly affected by duplex formation [35]. Binding of pyrene-labeled AS-1, AS-2 or AS-3 to the RNA resulted in enhancement of the pyrene fluorescence (Fig. 3). Fluorescence of random pyrene-labeled oligonucleotide was not affected by the RNA (data not shown). The association constants (K_x) for oligonucleotides AS-1, AS-2 and AS-3 derived from fluorescence titration data using the modified Shtern–Folmer equation are 10^6 M^{-1}, 0.87×10^7 M^{-1} and 0.7×10^6 M^{-1}, respectively.

4. Discussion

The key step in the design of antisense oligonucleotides is the identification of the optimal target sequences in the RNA. In the present study, we combined computer simulation with enzymatic probing to build a model of secondary structure of the *PGY1/MDR1* mRNA fragment and to identify the RNA regions that might be efficient targets for antisense oligonucleotides. We assumed that the investigated RNA fragment has the structure similar to that of the corresponding region in the full length *PGY1/MDR1* mRNA. This assumption is supported by studies of hybridization of antisense oligonu-

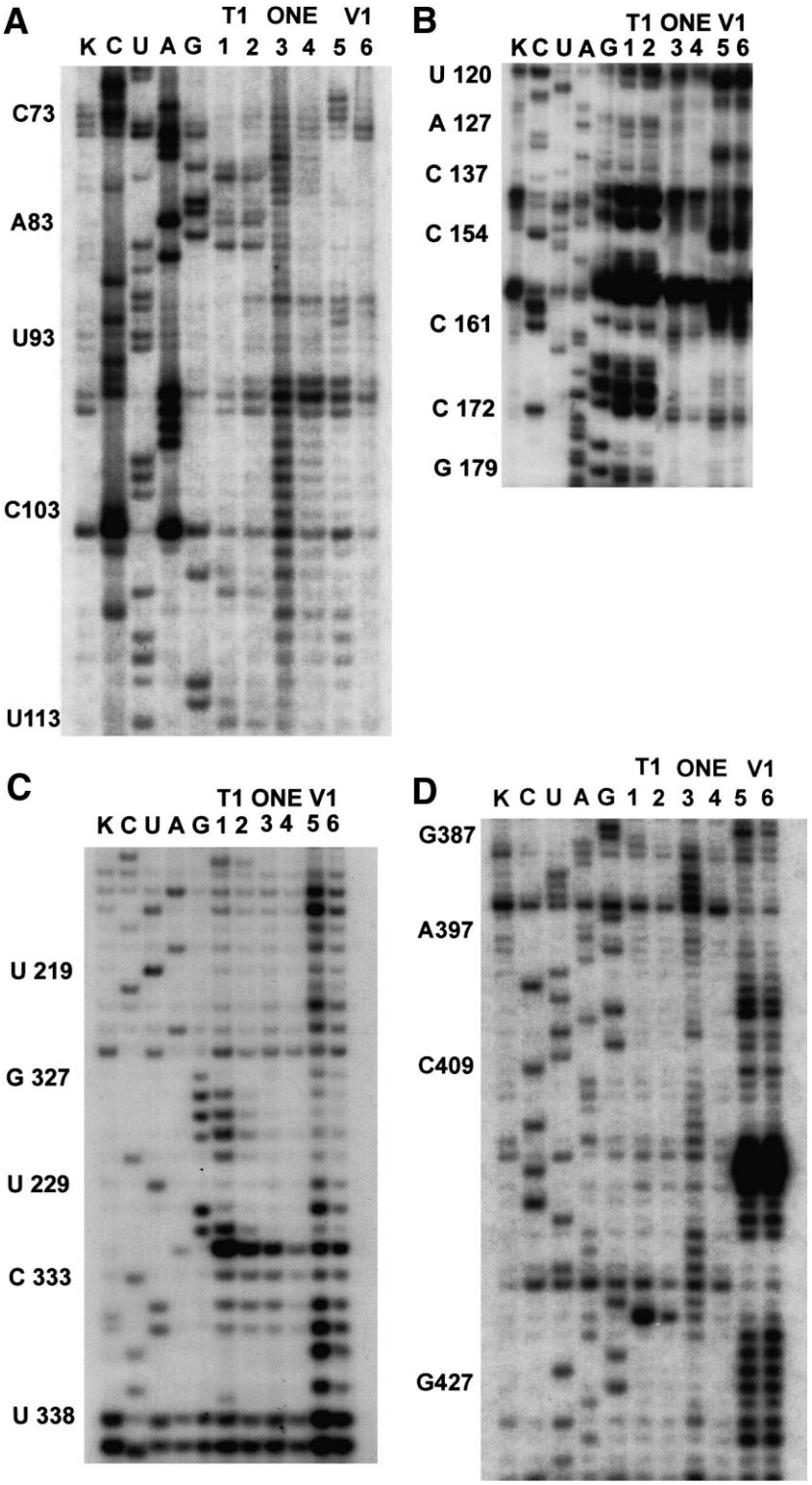

Fig. 1. Probing of the structure of in vitro transcript of human *PGY1/MDR1* RNA fragment with RNases T1, ONE and V1 in physiological conditions (50 mM HEPES, pH 7.0, containing 200 mM KCl, 5 mM $MgCl_2$). Autoradiographs of 6% denaturing PAGE fractionation of cDNA products obtained by primer-directed reverse transcription of RNase-treated and control RNA. A: Extension of ^{32}P-labeled oligonucleotide 130-RT, B: extension of ^{32}P-labeled oligonucleotide 240-RT, C: extension of ^{32}P-labeled oligonucleotide 340-RT, D: extension of ^{32}P-labeled oligonucleotide 450-RT. K: Incubation control. Lanes C, U, A, G, sequencing products generated by extension of the same primer in the presence of ddGTP, ddATP, ddTTP and ddCTP, respectively. Lanes 1–6, primer extension of in vitro transcribed *PGY1/MDR1* mRNA treated with RNases: 1, 2: RNase T1 (0.1–0.05 U/ml); 3, 4: RNase ONE (0.05–0.03 U/ml); 5, 6: RNase V1 (0.1–0.05 U/ml). *PGY1/MDR1* mRNA sequence is indicated on the left panel.

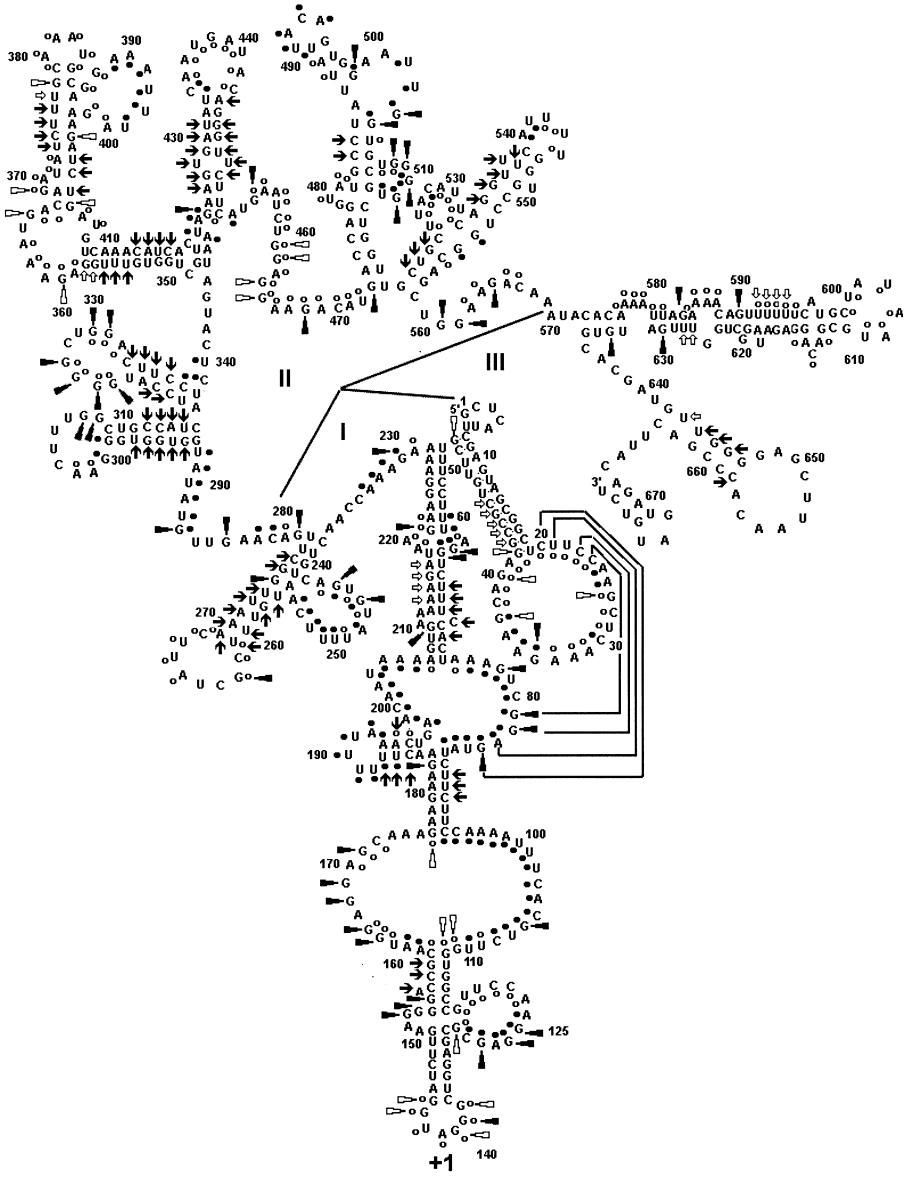

Fig. 2. Secondary structure of the 5′-terminal fragment of *PGY1/MDR1* mRNA. (●, ○) indicate sites strongly or weakly reactive to RNase ONE; (🡄, ⇦) indicate sites strongly or weakly reactive to RNase V1; (▶, ▷) indicate sites strongly or weakly reactive to RNase T1. Pseudoknott forming sequences are connected by lines.

cleotides with the long mRNA and its shortened versions [10]. There is the only computer-derived fold of full length *PGY1/MDR1* mRNA obtained using FOLD program, which finds a structure with minimum energy and with a maximum number of bases paired intramolecularly [36]. Results of these calculations show that *PGY1/MDR1* RNA is extensively folded: in the predicted model, 62% of the bases are paired. In some parts, the structure of the 5′-proximal region calculated in [36] seems to be similar to that shown in Fig. 2. Both structures are built of three domains. According to our data, the structure of the 5′-terminal fragment of *PGY1/MDR1* mRNA is more open and contains a number of loops of different nature. In the presented structure, the AUG codon is located in the octanucleotide loop (Fig. 2). This is in accordance with the available experimental data about accessibility of the initiation translation site to antisense oligonucleotides [9–11,35,37].

The proposed structure of *PGY1/MDR1* mRNA fragment is in agreement with published data on testing antisense oligonucleotides [9,11] and the data of the studies on hybridization of semi-random oligonucleotides library with *PGY1/MDR1* mRNA followed by cleavage with RNAse H [10]. The most efficient hybridization with the *PGY1/MDR1* mRNA was detected within the region 126–175 (A of AUG codon corresponds to position 141) that includes unstructured sequences and unstable secondary structure elements in the proposed model. Oligonucleotides complementary to sequences 117–137, 131–152, 162–181 of *PGY1/MDR1* mRNA were shown to suppress the P-gp function for 60–90% [10]. However, several attempts to inhibit *PGY1/MDR1* gene expression by antisense oligonucleotides failed [38]. Oligonucleotides complementary to the sequences 31–50, 57–76, 87–106, 177–196 demonstrated poor antisense activity [10]. According to our data, these oligonucleotides are

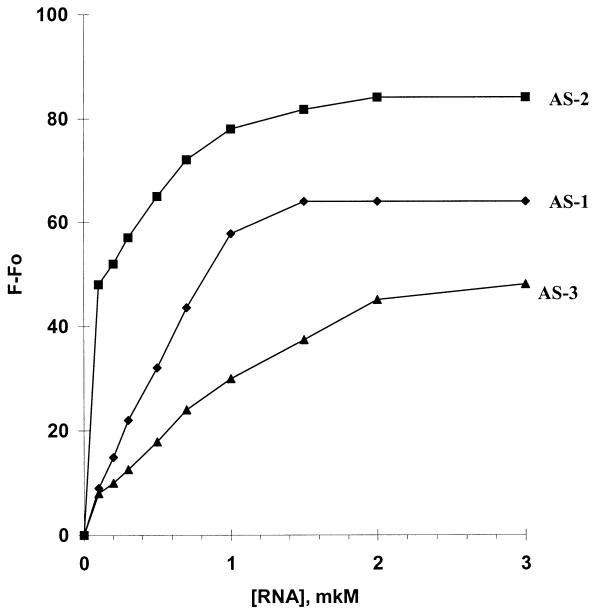

Fig. 3. Dependence of fluorescence of pyrene-labeled oligonucleotides AS-1, AS-2 and AS-3 on binding to the in vitro transcript of *PGY1/MDR1* mRNA at 37°C in 50 mM HEPES pH 7.5, 5 mM $MgCl_2$, 200 mM KCl, 0.5 mM EDTA. Oligonucleotide concentration was 5×10^{-7} M. Fo and F, fluorescence intensity (arbitrary units) of free and RNA bound pyrene-labeled oligonucleotide, respectively. Association constants were calculated from the presented curves using the modified Shtern–Folmer equation [30].

complementary to double-stranded regions of the *PGY1/MDR1* mRNA.

Antisense oligonucleotides AS-1, AS-2 and AS-3 were designed to target RNA in the structure shown in Fig. 2. Target sequences for the oligonucleotides contain 6–8 nucleotides long single-stranded regions to initiate the binding [32–34]. The tested oligonucleotides show quite an efficient hybridization: association constants (K_x) are 10^6 M^{-1}, 0.87×10^7 M^{-1} and 0.7×10^6 M^{-1} for oligonucleotides AS-1, AS-2 and AS-3, respectively. The obtained association constants are comparable with those of the tight binding antisense oligonucleotides that efficiently down regulate gene expression [34,39]. For example, the association constants for oligonucleotides that effectively bind and unfold the acceptor and TΨC stems of yeast $tRNA^{Phe}$ are within the range of 10^5 M^{-1} [32]. The most efficient binding is observed for oligonucleotide AS-2, complementary to the region +10 to +25 (150–165), which comprises two short single-stranded sequences separated by a short stem. AS-1 and AS-3 show similar binding efficiency. Their targets include single-stranded sequences adjacent to stem regions with mismatches. Antisense oligonucleotide [36] complementary to sequence +18 to +33, that is close to the target of oligonucleotide AS-2, was the only effective in down regulation of P-gp expression in MCF-7/ADR cells.

The obtained results evidence that the built model of the *PGY1/MDR1* mRNA fragment allows the prediction of the sequences accessible for efficient oligonucleotide hybridization. Derivatization of the identified antisense oligonucleotides with the reactive groups and groups providing efficient cellular uptake may result in the development of efficient inhibitors of *PGY1/MDR1* mRNA expression which might be of therapeutics value.

Acknowledgements: This work was supported by the Grant INTAS-RFBR 95-0653, Interdisciplinary grant of Siberian Branch of Russian Academy of Science, RFBR Grants N 96-15-97732 and 99-49559.

References

[1] Goldstain, L.J., Galski, H., Fojo, A., Willingham, M., Lai, A., Gazdar, A., Pirker, R., Green, A., Crist, W., Brodeur, G.M., Lieber, M., Cossman, J., Gottesman, M.M. and Pastan, I. (1989) J. Natl. Cancer Inst. 81, 116–124.
[2] Roninson, I.B. (1992) Biochem. Pharmacol. 43, 95–102.
[3] Damiani, D., Michieli, M., Michelutti, A., Melli, C. and Cerno, M. (1993) Anticancer Drugs 4, 178–180.
[4] List, A.F., Spier, C., Greer, J. and Phase, I. (1993) J. Clin. Oncol. 11, 1652–1660.
[5] Zalcberg, J.R., Hu, X.F. and Ching, M. (1991) Cancer Chemother. Pharmacol. 27, 290–294.
[6] Berman, E., Adams, M. and Osterndof, R. (1991) Blood 77, 818–825.
[7] Sikic, B.I. (1993) J. Clin. Oncol. 11, 1629–1635.
[8] Cook, P.D. (1993) in: Antisense Research and Applications (Crook, T. and Leableu, B., Eds.), pp. 149–187, CRC Press, Boca Raton, FL.
[9] Bouffard, D.Y., Ohkawa, T., Kijima, H. and Irie, A. (1996) Eur. J. Cancer 32A, 1010–1018.
[10] Ho, S.P., Britton, D.H., Stone, B.A., Behrens, D.L., Leffet, Hobbs, F.W., Miller, J.A. and Trainor, G.L. (1996) Nucleic Acids Res. 24, 1901–1907.
[11] Alahari, S.K. (1998) J. Pharmacol. Exp. Ther. 286, 419–428.
[12] Vickers, T.A. and Ecker, J. (1992) Nucleic Acids Res. 20, 3945–3953.
[13] Southern, E.M., Milner, N. and Mir, K.U. (1997) Ciba Found. Symp. 209, 38–46.
[14] Milner, N., Mir, K.U. and Southern, E.M. (1997) Nat. Biotechnol. 15, 537–541.
[15] Hakala, H., Heinonen, P., Iitia, A. and Lonnberg, H. (1997) Bioconjug. Chem. 8, 378–384.
[16] Ho, S.P., Bao, Y., Lesher, T., Malhorta, R., Ma, L.Y., Fluharty, S.J., Sakai (1998) Nat. Biotechnol. 16, 59–63.
[17] Lima, W.F., Brown-Driver, V., Fox, M., Hanecak, R. and Bruice, T.W. (1997) J. Biol. Chem. 272, 625–638.
[18] Matveeva, O., Felden, B., Audlin, S., Gestaland, R.F. and Atkins, J.F. (1997) Nucleic Acids Res. 25, 5010–5016.
[19] Mir, K.U. and Southern, E.M. (1999) Nat. Biotechnol. 17, 788–792.
[20] King, L.E. and Morrison, M. (1976) Anal. Biochem. 71, 223–230.
[21] Kostenko, E.V., Bibilashvilly, R.Sh., Vlassov, V.V. and Zenkova, M.A. (2000) Mol. Biol. (Moscow) 34, 67–78.
[22] Milligan, J.F., Groebe, D.R., Witherell, G.W. and Uhlenbeck, O.C. (1987) Nucleic Acids Res. 15, 8783–8798.
[23] Ehresmann, C., Baudin, F., Mougel, M., Romby, P. and Ebel, J.-P. (1987) Nucleic Acids Res. 15, 9109–9128.
[24] Bruice, T.W. and Lima, W.F. (1997) Biochemistry 36, 5004–5019.
[25] Vassilenko, S.K. and Rythe, V.C. (1975) Biokhimiya 40, 578–582.
[26] Lempereur, L., Nicoloso, M., Riehl, N., Ehresmann, C., Ehresmann, B. and Bachellerie, J.-P. (1985) Nucleic Acids Res. 13, 8339–8357.
[27] Devereux, J., Haeberli, P. and Smithies, O. (1984) Nucleic Acids Res. 12, 387–395.
[28] Abrahams, J.P., van den Berg, M., van Batenburg, E. and Pleij, C. (1990) Nucleic Acids Res. 18, 3035–3044.
[29] Zarytova, V.F., Godovicova, T.S., Kutiavin, I.V. and Khalimskaya, L.M. (1987) in: Biophosphates and their Analogues, Synthesis, Structure, Methabolism and Activity (Bruzik, K.S. and Stec, W.S., Eds.), pp. 149–164, Elsevier, Amsterdam.
[30] Lakovich, J.R. (1983) in: Principles of Fluorescence Spectroscopy, pp. 270–275, Plenum Press, NY.
[31] Hosaka, H., Sakabe, I., Sakamoto, K., Niimi, T., Yokoyama, S. and Takaku, H. (1994) Biochem. Biophys. Acta 1218, 351–356.
[32] Petyuk, V.A., Zenkova, M.A., Giege, R. and Vlassov, V.V. (1999) FEBS Lett. 444, 217–221.
[33] Petyuk, V.A., Zenkova, M.A., Giege, R. and Vlassov, V.V. (1999) Nucleosides Nucleotides 18, 1459–1461.
[34] Ecker, D.J. (1993) in: Antisense Research and Applications

(Crook, T. and Leableu, B., Eds.), pp. 387–414, CRC Press, Boca Raton, FL.
[35] Dobricov, M.I., Gaidamakov, S.A., Koshkin, A.A., Gainutdinov, T.I., Luk'yanchuk, N.P., Shishkin, G.V. and Vlassov, V.V. (1997) Bioorg. Chem. (Moscow) 23, 191–199.
[36] Jaroszewski, J.W., Kaplan, O., Syi, J.L., Sehested, M., Faustino, P.J. and Cohen, J.S. (1990) Cancer Commun. 2, 287–294.
[37] Corrias, M.V. and Tonini, G.P. (1992) Anticancer Res. 12, 1431–1438.
[38] Chao, L., Qureshi, A., Ding, X. and Shan, Y. (1996) Clin. Sci. 91, 93–98.
[39] Freier, S.M. (1993) in: Antisense Research and Application (Crook, T. and Leableu, B., Eds.), pp. 67–81, CRC Press, Boca Raton, FL.